

RESEARCH ARTICLE

Multi-physical field control piezoelectric inkjet bioprinting for 3D tissue-like structure manufacturing

Supplementary File

1. Theoretical analysis of force exerted on microdroplets suspended in air

The microdroplet is influenced by gravity and air resistance. The microdroplet is influenced by gravity and air resistance. In fluid dynamics, the resistance of a spherical body moving through a fluid can be calculated using Stokes' law if the Reynolds number is small. Thus, the air resistance is calculated using Stockton's law in Equation S1:¹

$$F = 6\pi\eta\nu R \quad (S1)$$

where F , η , ν , and R are the air resistance, viscosity coefficient, viscosity, and radius, respectively. F is calculated as approximately 2.5×10^{-8} N.

The gravity of the microdroplet is determined in Equation S2:

$$G = \frac{4}{3}\pi R^3 \rho g \quad (S2)$$

where G , R , ρ , and g are the gravity, radius, density, and gravitational acceleration, respectively. G is calculated as approximately 2.65×10^{-8} N. After calculation, air resistance and gravity are approximately equal to each other. Therefore, the acceleration of microdroplets in the air is relatively small, and the influence of air resistance and gravity can be ignored. It has been confirmed through microdroplet photography experiments that the variation in microdroplet velocity at different positions is very small.

2. 3% and 10% GelMA printability testing experiments

This study aims to expand the scope of the proposed method by conducting printability tests of GelMA at

different concentrations. Specifically, printability tests were conducted on 3% and 10% GelMA, which are widely adopted concentrations in printing experiments. Our previous experiment using 5% GelMA indicated that the control laws of microdroplet velocity and diameter remain the same due to the energy storage modulus, loss modulus, and viscosity approaching zero at 37°C in the printing head with different concentrations of GelMA. The temperature field is controlled by the upper cover to control the air temperature, and the control law of the air temperature controlling microdroplet temperature remains basically the same. Only the gel point of GelMA with varying concentrations has changed.

In our experiments, we first tested the rheological properties of 3% and 10% GelMA. Figure S1 shows the rheological test results of 3% GelMA, and its gel point is 12°C. According to the printing experiment of 5% GelMA, the printable temperature range should be near the gel point. After calculation, it was found that the microdroplet temperature decreased from 37°C to 12°C, and the air temperature was already close to 0°C. In order to avoid cell death, the air temperature cannot be lower than 0°C, meaning that the microdroplet temperature cannot be lower than 12°C. After experimental photography, if the final forming temperature of the microdroplet was higher than 13°C, the microdroplet would be in the liquid phase, as shown in Figure S1B-I. When the microdroplet is in the range of 12°C to 13°C, it will appear as a printable phase, as shown in Figure S1B-II. When the microdroplet temperature is below 12°C, the air temperature is already below 0°C and is not suitable for printing cells. But the microdroplet is still in the printable phase, as shown in the lower half of Figure S1B-II. When the temperature is lower, the microdroplet will bulge higher after forming. According to the previous speed and diameter, as well as the temperature control calculation, we also obtained the fitting surface of the 3% GelMA printable rule as shown in Figure S1C. The air temperatures on the surface for printing

were different depending on the microdroplet speeds and diameters. The final microdroplet assembly temperature can be controlled near the gel point to complete printing. To print cells, data above the 0°C plane should be selected.

Similarly, we also tested the rheological properties of 10% GelMA, as shown in Figure S1D. Its gel point is 21°C, the printable range is from 17°C to 22°C, and the microdroplet assembly temperature in this range is printable phase as shown in Figure S1E-II. When the assembly temperature is above 22°C, the liquid phase as shown in Figure S1E-I is formed, and below 17°C, the gel as shown in Figure S1E-III is formed. The resulting 10% GelMA printable surface is shown in Figure S1F. Through supplementary experiments, we also found that the printable range of 5% GelMA can be extended to 12°C–17°C, which has been updated in the article.

Based on our GelMA experiments with different concentrations, our findings suggest that the basic formulas of temperature field control and pressure field control presented in this article can be extended to other GelMA printing. The rheological properties of GelMA

need to be measured, and the final assembly temperature of microdroplets can be controlled near the gel point using the MFCPIB method for printing, which is of great significance to the research and application of GelMA inkjet bioprinting.

3. Formula derivation process

3.1. Pressure variation acoustoelectric analog capacitor discharge

By converting acoustic pressure wave oscillation problems into electrical oscillation problems, the difficulty of process analysis and modeling can be greatly simplified.² During the process of analogy, the viscous force and compressibility of the piezoelectric printhead are characterized by resistance and capacitance. The similarity between the physical processes of pressure release and capacitor discharge is used to liken the process of pressure change to the process of capacitor charging and discharging.^{3,4} The pressure change at the nozzle after spraying droplets is investigated, as shown in the circuit diagram below:

Circuit equation is given by Equation S3:

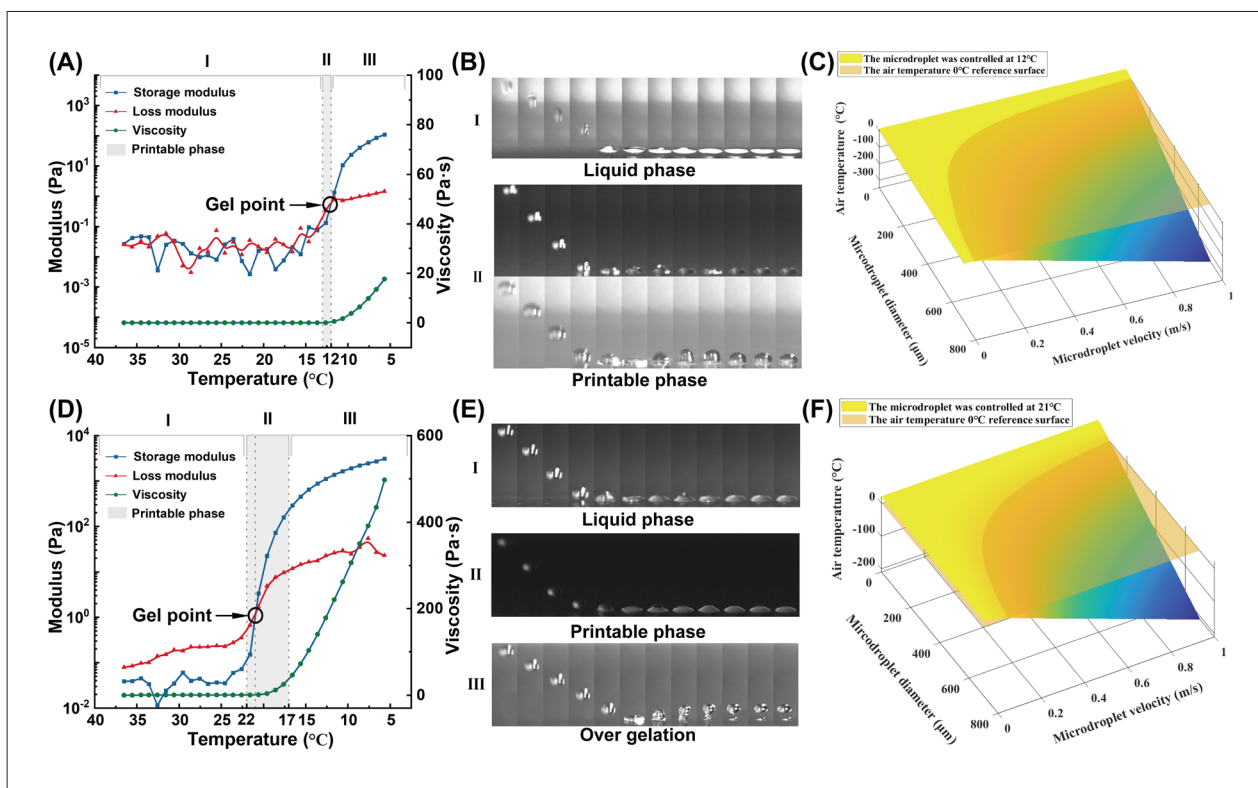


Figure S1. Controlling and optimizing the temperature field for varying concentrations of GelMA. (A) Rheological properties of 3% GelMA. (B) Observation of 3% GelMA microdroplet formation. (C) Summary of the MFCPIB relationship for 3% GelMA. (D) Rheological properties of 10% GelMA. (E) Observation of 10% GelMA microdroplet formation. (F) Summary of the MFCPIB relationship for 10% GelMA.

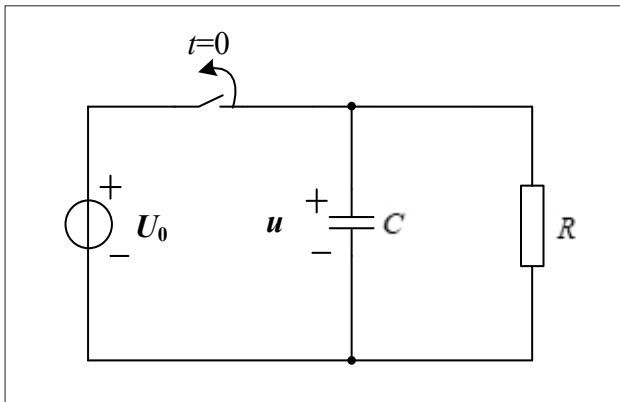


Figure S2. Circuit diagram.

$$\left\{ \begin{aligned} RC \frac{du(t)}{dt} + u(t) &= 0 \quad t > 0 \\ u(0) &= U_0 \end{aligned} \right\} \tag{S3}$$

The solution of the above equation is as follows:

$$u(t) = U_0 e^{-\frac{t}{RC}} \quad t \geq 0 \tag{S4}$$

So, the pressure P is

$$P = Ae^{(-t/T)} \tag{S5}$$

3.2. Effect of pulse width on diameter and velocity

According to Equation III in the main article, the pressure P on the fluid element is given by:

$$P = Ae^{(-t/T)} \tag{S5}$$

where P , A , t , and T are the pressure, coefficient, time, and time constant, respectively. The acceleration a is defined by **Equation S6**:

$$a = \frac{Ae^{(-t/T)}}{\rho} \tag{S6}$$

The velocity V is obtained by integrating the fluid element acceleration a :

$$V = \int \frac{Ae^{(-t/T)}}{\rho} dt = -\frac{AT}{\rho} e^{(-t/T)} + B \tag{S7}$$

where P , A , B , t , T , and ρ are the pressure, coefficient, coefficient, time, time constant, and density, respectively. The fluid element diameter D is the integral of the velocity V , as shown in **Equation S8**:

$$D = \int \frac{AT}{\rho} e^{(-t/T)} + B dt = +\frac{AT^2}{\rho} e^{(-t/T)} + C \tag{S8}$$

where P , A , B , C , t , T , and ρ are the pressure, coefficient, coefficient, coefficient, time, time constant, and density, respectively.

References

1. Zwanzig R. Hydrodynamic fluctuations and Stokes' law friction. *J Res Natl Bur Stan Sect B Math Math Phys.* 1964;68B:143. doi: 10.6028/jres.068B.019
2. He M, Sun L, Hu K, Zhu Y, Ma L, Chen H. Drop-on-demand inkjet printhead performance enhancement by dynamic lumped element modeling for printable electronics fabrication. *Math Probl Eng.* 2014;2014:1-16. doi: 10.1155/2014/270679
3. Shah MA, Lee D-G, Lee BY, Kim NW, An H, Hur S. Actuating voltage waveform optimization of piezoelectric inkjet printhead for suppression of residual vibrations. *Micromachines.* 2020;11:900. doi: 10.3390/mi11100900
4. Gallas Q, Sheplak M, Kaysap A, et al. Lumped element modeling of piezoelectric-driven synthetic jet actuators. 40th AIAA Aerospace Sciences Meeting & Exhibit. 2002. doi: 10.2514/6.2002-125